Computer Vision and Image Understanding

Extracting Group Transformations from Image Moments

Jun Sato and Roberto Cipolla
Department of Engineering, University of Cambridge, Cambridge CB2 1PZ, England
Received June 1997; accepted May 1998

Image distortion induced by the relative motion between an observer and the scene is an important cue for recovering the motion and the structure of the scene. It is known that the distortion in images can be described by transformation groups, such as Euclidean, affine and projective groups. In this paper, we investigate how the moments of image curves are changed by group transformations, and we derive a relationship between the change in image moments and the invariant vector fields of the transformation groups. The results are used to formalise a method for extracting invariant vector fields of affine transformations from changes in the moments of orientation of curve segments in images. The method is applied to realtime robot visual navigation task.

1 Introduction

Recent progress in computer vision has revealed the close relationships between the class of objects in images and *transformation groups* [21].

If an object is a surface of revolution and if it is projected in the image center, then the corresponding symmetric pair of contour curves of the object in the image can be described by a transformation of the Euclidean group as shown in Fig. 1 (a). If a planar object has bilateral symmetry viewed under weak perspective, the corresponding contour curves of the object in an image can be described by a transformation of the special affine group [11, 28] (see Fig. 1 (b)). The corresponding contour curves of a 3D bilateral symmetry such as a butterfly are related by a transformation of the general affine group [24] (see Fig. 1 (c)).

In structure from motion, the image distortion caused by the relative motion between the observer and the scene can be described by an affine transformation under *weak perspective* assumption [16, 15] (see Fig. 1 (e)). If the viewer motion is restricted to a translation along the

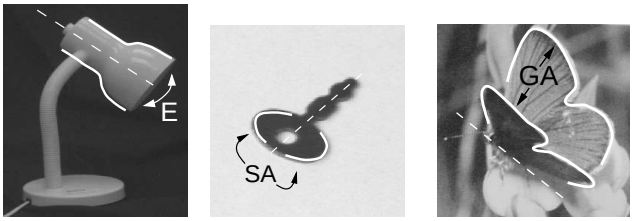

(a) Euclidean (b) special affine (c) general affine

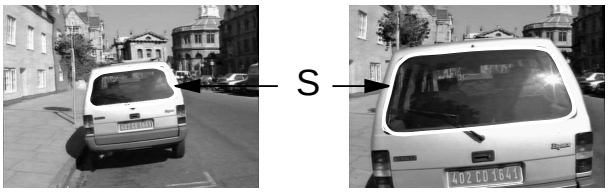

(d) similarity

(e) general affine

Figure 1: **Image distortion and transformation groups.** A symmetric pair of contour curves (white curves) of (a) a surface of revolution, (b) planar bilateral symmetry and (c) 3D bilateral symmetry can be described by Euclidean, special affine (equi-affine) and general affine (proper affine) transformations under the weak perspective assumption. The image distortion caused by the relative motion between the observer and the scene can also be described by group transformations as shown in (d) and (e). The original images in (a) and (b) have been provided courtesy of Tat-Jen Cham.

optical axis towards the object, the image distortion can be described by the similarity group [7] (see Fig. 1 (d)). Thus, extracting group transformations in images is an integral part for object recognition and motion extraction.

Unfortunately, the existing methods for computing group transformations suffer from the requirement for corresponding image features [13, 22, 26], limitation to the amount of image motions [8] and/or high sensitivity to noise [1, 3]. If the interest areas (focus of attention) in images are identified, moment based methods [4, 9, 7, 12, 25] are useful. They do not require correspondences of individual image features, do not suffer from small image noise and allow large image motions. Unfortunately, the conventional analyses in the moment based methods are limited to specific transformation groups [7, 12]. In this paper, we aim to formalise a method for extracting *general* group transformations in images from changes in image moment.

For this objective, we first review the Lie group theory [23, 10], which has recently been imported to computer vision research [8, 14, 29], and investigate how the change in image moments under general group transformations can be described by the basis vector fields of the group. Especially, we will exploit a prolonged space [23], an extended space for derivatives, and analyse the change in values of functions with derivatives explicitly from a geometric point of view. The results of the analysis are exploited for formalising a method for computing group transformations from the change in image moments. The affine case is especially studied, and a method for computing affine transformations from the change in image moments is formalised.

2 Geometric Analysis of Differential Image Properties

We first review a geometric approach for analysing differential properties of images. We consider that the derivatives are added dimensions of the space and are transformed as geometric objects. The methodology described in this section is an established area in mathematics [23], and thus the contents of this section are a review of this field which is, as shown in the later section, useful for investigating differential properties of images in computer vision.

2.1 Group Transformation and Vector Field

Let G be a Lie group, that is a group which carries the structure of a smooth manifold in such a way that both the group operation (multiplication) and the inversion are smooth maps [23]. Transformation groups such as rotation, Euclidean, affine and projective groups are Lie groups. Consider vector fields on G. There exist certain distinguished vector fields, i.e. *right (or left) invariant* vector fields, $\mathbf{w}$, on G, which form a finite dimensional vector space called the *Lie algebra* of G. Geometrically, the Lie algebra of G is identified as the tangent space to the manifold, G, at the identity. Consider an m-parameter Lie group, G. Since the Lie algebra of G is an m dimensional vector space, any vector field, $\mathbf{w}$, in the Lie algebra can be described by a linear combination of m basis vector fields, $\mathbf{w}_i (i = 1, \cdots, m)$, of the Lie algebra. The flow generated by $\mathbf{w}$ through the identity is a so called *one-parameter subgroup* of G, and there is a one-to-one correspondence between one-parameter subgroups of G and one dimensional subspaces of the Lie algebra.

We next consider the action of an m-parameter Lie group, G, on a manifold, M, which is in our case the image plane $\mathbf{R}^2$ with coordinates of x and y. Take the m one parameter subgroups corresponding to m basis vector fields of the Lie algebra of G. These act on M and induce m vector fields, $\mathbf{v}_i$, on M:

$$\mathbf{v}_i = \xi_i \frac{\partial}{\partial x} + \eta_i \frac{\partial}{\partial y} \qquad (i = 1, \cdots, m) \tag{1}$$

where, ξ_i and η_i are functions of x and y. These are the basis vector fields on M, and every vector field, $\mathbf{v}$, induced by one parameter subgroups of G can be expressed as a linear combination of the basis vector fields, $\mathbf{v}_i$, as follows:

$$\mathbf{v} = \sum_{i=1}^{m} a_i \mathbf{v}_i \tag{2}$$

where, a_i is a coefficient of ith vector field. To extract local group transformations is the same as to identify the coefficients, $a_i (i = 1, ..., m)$, of the basis vector fields.

As we will see in the next section, the vector field described in (1) acts as a differential operator of the Lie derivative.

2.2 Lie Derivatives

Consider a function, $F(x, y)$, of x and y to be defined on the image plane $\mathbf{R}^2$. As G acts on a point on the image plane, the x and y coordinates of the point change, and thus the value of the function, $F(x, y)$, also changes. It is known [23] that the infinitesimal change in value, δF, of the function, F, under the flow induced by a vector field, $\mathbf{v}$, can be computed by the Lie derivative of F with respect to $\mathbf{v}$ as follows:

$$\delta F = \pounds_{\mathbf{v}}[F(x, y)]$$

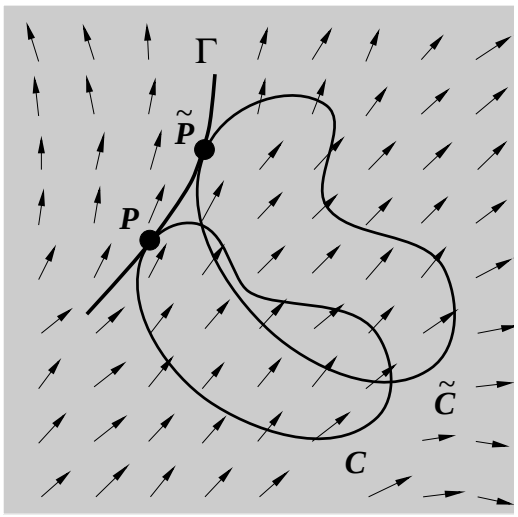

Figure 2: **The vector field, $\mathbf{v}$, and an integral curve, Γ.** The curve $\boldsymbol{C}$ is transformed to $\widetilde{\boldsymbol{C}}$ by a group transformation, so that the point $\boldsymbol{P}$ on the curve is transformed to $\widetilde{\boldsymbol{P}}$. The orbit of the point caused by a group transformation coincides with the integral curve, Γ, of the vector field at the point, $\boldsymbol{P}$.

where, $\pounds_{\mathbf{v}}[\cdot]$ denotes Lie derivative with respect to a vector field, $\mathbf{v}$. Since F is a scalar function, the Lie derivative is the same as the directional derivative with respect to $\mathbf{v}$:

$$\delta F = \mathbf{v}[F(x,y)]$$

Thus, we can compute the infinitesimal change in function caused by the flow induced by a vector field $\mathbf{v}$ by using the differential operator defined by (1).

Up to now we assumed that F is a function of x and y. In the next section, we introduce an important concept known as the *prolongation* of vector fields, and consider the changes in functions of x, y and the derivatives of y with respect to x under the vector fields.

2.3 Prolongation of Vector Fields

The prolongation is a method for investigating the differential world from a geometric point of view. Let a smooth curve, $\boldsymbol{C}$, on the image plane $\mathbf{R}^2$ be described by an independent variable x and a dependent variable y with a smooth function f as follows:

$$y = f(x)$$

The curve, $\boldsymbol{C}$, is transformed to $\widetilde{\boldsymbol{C}}$ under the flow induced by a vector field, $\mathbf{v}$, as shown in Fig. 3. Consider a jth order prolonged space, whose coordinates are x, y and derivatives of y with respect to x up to jth order, so that the prolonged space is $j+2$ dimensional. The curves, $\boldsymbol{C}$ and $\widetilde{\boldsymbol{C}}$, in 2D space are prolonged and described by curves, $\boldsymbol{C}^{(j)}$ and $\widetilde{\boldsymbol{C}}^{(j)}$, in the $j+2$ dimensional prolonged space. The prolonged vector field, $\mathbf{v}^{(j)}$, is a vector field in $j+2$ dimension, which carries the prolonged curve, $\boldsymbol{C}^{(j)}$, to the prolonged curve, $\widetilde{\boldsymbol{C}}^{(j)}$ explicitly as shown in Fig. 3. More precisely, the jth order prolongation, $\mathbf{v}^{(j)}$, of a vector field, $\mathbf{v}$, is defined so that it transforms the jth order derivatives, $y^{(j)}$, of a function, $y = f(x)$, into the corresponding jth order derivatives, $\widetilde{y}^{(j)}$, of the transformed function $\widetilde{y} = \widetilde{f}(\widetilde{x})$ geometrically.

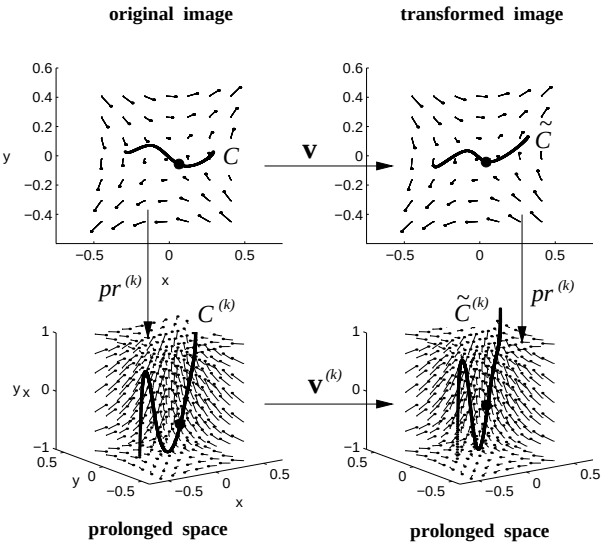

Figure 3: **Prolongation of a vector field.** The jth order prolonged vector field, $\mathbf{v}^{(j)}$ transforms jth order derivatives of y into jth order derivatives of $\widetilde{y}$. That is the prolonged curve, $\boldsymbol{C}^{(j)}$, is transformed into the prolonged curve, $\widetilde{\boldsymbol{C}}^{(j)}$, by the prolonged vector field, $\mathbf{v}^{(j)}$. This enables us to investigate derivatives of functions geometrically. $pr^{(j)}$ denotes jth order prolongation. This figure illustrates the first order prolongation ($j=1$).

Let $\mathbf{v}_i, (i = 1,..,m)$ be m basis vector fields on M. The jth prolongation, $\mathbf{v}^{(j)}$, of a vector field, $\mathbf{v}$, can be described by a sum of jth prolongations, $\mathbf{v}_i^{(j)}$, of the basis vector fields, $\mathbf{v}_i$, as follows:

$$\mathbf{v}^{(j)} = \sum_{i=1}^{m} a_i \mathbf{v}_i^{(j)} \tag{3}$$

where as before a_i is the coefficient of the ith basis vector field. Consider a vector field, $\mathbf{v}_i$, defined by (1). Then, its first and second prolongations, $\mathbf{v}^{(1)}$, $\mathbf{v}^{(2)}$, are computed as follows [23]:

$$\mathbf{v}_i^{(1)} = \mathbf{v}_i + (D_x(\eta_i - \xi_i y_x) + \xi_i y_{xx})\frac{\partial}{\partial y_x} \tag{4}$$

$$\mathbf{v}_i^{(2)} = \mathbf{v}_i^{(1)} + (D_x^2(\eta_i - \xi_i y_x) + \xi_i y_{xxx})\frac{\partial}{\partial y_{xx}} \quad (5)$$

where D_x and D_x^2 denote the first and the second total derivatives with respect to x, and y_x, y_{xx}, y_{xxx} denote the first, second and the third derivatives of y with respect to x.

Let $F(x, y, y^{(j)})$ be a function of x, y and derivatives of y with respect to x up to jth order, which is denoted by $y^{(j)}$. Since the prolongation describes how the derivatives are going to change, the infinitesimal change in function, δF, under the flow induced by a vector field, $\mathbf{v}$, can be computed by using the prolongation as follows [23]:

$$\delta F = \mathbf{v}^{(j)}[F(x, y, y^{(j)})] \quad (6)$$

Note that we require only the same order of prolongation as that of the function, F.

3 Change in Moments under Group Transformations

In this section, we investigate how the moments in images vary under group transformations by applying the prolonged vector fields introduced in the last section. We first analyse the change in arc-length and orientation of a tangent vector of an image curve under vector fields of a Lie group.

3.1 Change in Orientation under Vector Field

Consider an image curve, $\boldsymbol{C}$, to be described by an independent variable, x, and a dependent variable, y, with a smooth function, f, as before. Then, the orientation, φ, of a tangent vector of the curve can be described by:

$$\sin\varphi = y_x(1 + y_x^2)^{-\frac{1}{2}} \quad (7)$$

$$\cos\varphi = (1 + y_x^2)^{-\frac{1}{2}} \quad (8)$$

where y_x denotes the first derivative of y with respect to x as before. As we have seen in the last section, the jth order derivatives are transformed by the jth order prolongations of the vector fields. Since, as shown in (7), φ is a function of the first derivative, y_x, the infinitesimal change in orientation $\delta\varphi$ caused by a vector field, $\mathbf{v}$, can be described by using the first order prolongation (4) as follows:

$$\begin{aligned}\delta\varphi &= \mathbf{v}^{(1)}[\varphi] \\ &= \sum_{i=1}^{m} a_i(\mathbf{v}_i[\varphi] + (D_x(\eta_i - \xi_i y_x) + \xi_i y_{xx})\frac{\partial\varphi}{\partial y_x}) \\ &= \sum_{i=1}^{m} a_i(D_x(\eta_i - \xi_i y_x) + \xi_i y_{xx})(1 + y_x^2)^{-1} \quad (9)\end{aligned}$$

where, we have used the derivative of φ with respect to y_x for the last equation in (9). Note we do not need prolongations higher than the first in this case.

3.2 Change in Arc-Length under Vector Field

Next, we investigate how the Euclidean arc-length changes under vector fields. The Euclidean arc-length, v, is described by an Euclidean metric, g, and the differential dx as follows:

$$dv = g dx \quad (10)$$

where:

$$g = (1 + y_x^2)^{\frac{1}{2}} \quad (11)$$

Since the metric, g, is described by first order derivatives of y with respect to x, the infinitesimal change in arc-length, δdv, caused by the vector field, $\mathbf{v}$, is derived by computing the Lie derivative of dv with respect to the first order prolongation of the vector field, $\mathbf{v}^{(1)}$, as follows:

$$\begin{aligned}\delta dv &= \mathbf{v}^{(1)}[dv] \\ &= \sum_{i=1}^{m} a_i(\mathbf{v}_i^{(1)}[\,g\,] + g\frac{d\xi_i}{dx})dx \\ &= \sum_{i=1}^{m} a_i(y_x(D_x(\eta_i - \xi_i y_x) + \xi_i y_{xx})(1 + y_x^2)^{-1} + \frac{d\xi_i}{dx})dv\end{aligned} \quad (12)$$

where, we used the derivative of g with respect to y_x for the last equation in (12). Note again the prolongations higher than the first are not required.

3.3 Change in Curvature under Vector Field

We now consider how the Euclidean curvature changes under vector fields. The Euclidean curvature, κ, is described by:

$$\kappa = y_{xx}(1 + y_x^2)^{-\frac{3}{2}}$$

Since κ is made of derivatives up to the second, the infinitesimal change in curvature, $\delta\kappa$, caused by the vector field, $\mathbf{v}$, is derived by using the second prolongation as follows:

$$\begin{aligned}\delta\kappa &= \mathbf{v}^{(2)}[\kappa] \\ &= \mathbf{v}_i^{(1)}[\kappa] + (D_x^2(\eta_i - \xi_i y_x) + \xi_i y_{xxx})\frac{\partial\kappa}{\partial y_{xx}} \quad (13)\end{aligned}$$

These results will be used in the following sections for deriving the relationship between the coefficients of the vector field, a_i, and the change in moments.

3.4 Change in Moments under Vector Field

Consider the texture in an image to have oriented elements with distribution of orientation, $\rho(\varphi)$ (i.e. density function with respect to the orientation, φ, of the texture element). Suppose F is a function of x, y and the derivatives of y with respect to x up to jth order. The moment, I, of the function F is defined by $I = \int_0^{2\pi} F\rho(\varphi)d\varphi$. If the image features are described by a parameterised curve, $\boldsymbol{C}$, the moment I can also be computed by integrating a function F with respect to an Euclidean arc-length, dv, along the curve, $\boldsymbol{C}$:

$$I = \int_C F dv \tag{14}$$

In this case, the distribution of orientation, ρ, can be described by a Euclidean curvature, κ, as follows:

$$\rho = \frac{dv}{d\varphi} = \frac{1}{\kappa}$$

In the remaining part of this paper, we assume that the image features can be described by parameterised curves which are differentiable as many times as required. (As we will describe in the later experiments, these parameterised curves can be derived by fitting B-spline functions to image data.)

Since the Lie derivative describes the infinitesimal change in function, the infinitesimal change in moment δI caused by a vector field, $\mathbf{v}$, is described by the Lie derivative of I with respect to the vector field, $\mathbf{v}$:

$$\delta I = \mathbf{v}^{(j)}[\,I\,] \tag{15}$$

Substituting (14) into (15), we have the following equation of change in moments:

$$\delta I = \int_C \mathbf{v}^{(j)}[F]dv + F\mathbf{v}^{(1)}[dv] \tag{16}$$

where, we have exploited 1st and jth order prolongations of the vector field $\mathbf{v}$, since dv and F are made of first and jth order derivatives respectively.

3.5 Change in Directional Moment and Vector Field

Since, as described in section 2.3, a prolonged vector field transforms derivatives explicitly, we can use not only algebraic functions, but also differential functions for F in equation (16). This enables us to derive the relationship between the vector fields and the change in moments of orientation of texture in images.

Suppose F takes nth order trigonometric functions of φ, that is $\sin n\varphi$ and $\cos n\varphi$. The nth order trigonometric moments can be defined by [9, 19]:

$$I_{\sin n\varphi} = \int_C \sin n\varphi dv \tag{17}$$

$$I_{\cos n\varphi} = \int_C \cos n\varphi dv \tag{18}$$

These are the moments of orientation of texture in images. In the following part of this paper, we call the above trigonometric moments *directional moments* to make its physical meaning clear. Substituting $\sin n\varphi$ and $\cos n\varphi$ for F in (16), gives the infinitesimal change in directional moments as follows:

$$\delta I_{\sin n\varphi} = \int_C (n\mathbf{v}^{(1)}[\varphi]\cos n\varphi + \frac{\mathbf{v}^{(1)}[dv]}{dv}\sin n\varphi)dv \tag{19}$$

$$\delta I_{\cos n\varphi} = \int_C (-n\mathbf{v}^{(1)}[\varphi]\sin n\varphi + \frac{\mathbf{v}^{(1)}[dv]}{dv}\cos n\varphi)dv \tag{20}$$

where, $\mathbf{v}^{(1)}[\varphi]$ and $\mathbf{v}^{(1)}[dv]$ are as investigated in (9) and (12). In (19) and (20), we have m unknowns, i.e. m coefficients of basis vector fields, $a_i, (i = 1, 2, \cdots, m)$. Thus, if we have q_1 order moments and $m \leq 2q_1$, we can compute these coefficients, a_i, uniquely.

3.6 Change in Curvature Moment and Vector Field

We next consider the change in curvature moments. We define nth order curvature moment, I_{κ^n}, so that F takes nth order curvature function, κ^n, as follows:

$$I_{\kappa^n} = \int_C \kappa^n dv \tag{21}$$

Substituting κ^n for F in (16), we have the infinitesimal change in curvature moments as follows:

$$\delta I_{\kappa^n} = \int_C (n\kappa^{n-1}\mathbf{v}^{(2)}[\kappa] + \frac{\mathbf{v}^{(1)}[dv]}{dv}\kappa^n)dv \tag{22}$$

The variation of n in (22) provides interesting properties as it will be described in section 4.5. We have again m unknowns, i.e. $a_i (i = 1, 2, \cdots, m)$ in (22). Thus, if we have q_2 order moments and $m \leq q_2$, we can compute these coefficients, a_i, uniquely. In the following part of this paper, we concentrating on the affine case, and derive a method for computing the affine transformations from these image moments.

4 Changes in Moments under Affine Transformations

Up to now we have derived the change in moments under vector fields of general Lie groups. We now consider a specific Lie group, the general affine group, and derive the relationship between the change in moments and an affine transformation.

4.1 Affine Transformation and Affine Vector Field

A 2D affine transformation consists of a 2×2 invertible matrix, $A \in GL(2)$, and a 2×1 vector, $\boldsymbol{t} \in \mathbf{R}^2$, and transforms $\boldsymbol{x} \in \mathbf{R}^2$ to $\widetilde{\boldsymbol{x}} \in \mathbf{R}^2$ as follows:

$$\widetilde{\boldsymbol{x}} = A\boldsymbol{x} + \boldsymbol{t}$$

where, the symbol, $\widetilde{\ }$, denotes the components transformed by an affine transformation. If we consider relative components, $\Delta\boldsymbol{x} = \boldsymbol{x}_1 - \boldsymbol{x}_0$ $(\boldsymbol{x}_0, \boldsymbol{x}_1 \in \mathbf{R}^2)$, the affine transformation can be simplified as follows:

$$\Delta\widetilde{\boldsymbol{x}} = A\Delta\boldsymbol{x}$$

If $\boldsymbol{x}(p)$ is a point on a curve parameterised by p, the derivative of $\boldsymbol{x}$ with respect to p can also be transformed in the same simple manner [20]:

$$\widetilde{\boldsymbol{x}}_p = A\boldsymbol{x}_p$$

where, $\widetilde{\boldsymbol{x}}_p$ and $\boldsymbol{x}_p$ denote the derivatives of $\widetilde{\boldsymbol{x}}$ and $\boldsymbol{x}$ with respect to p. In the following part of this paper, we simply consider the linear part of the affine transformation, A, and neglect the translation component, $\boldsymbol{t}$. If the determinant, $[A]$, of the matrix A is equal to one, the transformation is called a special affine (equi-affine) transformation. A general (proper) affine transformation takes any real value except zero for the determinant $[A]$.

Consider a smooth planar curve, $\boldsymbol{C} \in \mathbf{R}^2$, to be transformed to $\widetilde{\boldsymbol{C}} \in \mathbf{R}^2$ by an affine transformation, A:

$$\widetilde{\boldsymbol{C}} = A\boldsymbol{C} \tag{23}$$

It is well known that if the image distortion caused by the affine transformation is small, the affine transformation can be decomposed into four components [7, 14, 17], that is divergence, curl and two components of deformation as shown in Fig. 5 (a2), (b2), (c2) and (d2). The affine vector field is described by the linear combination of these four components as follows:

$$\mathbf{v} = a_1\mathbf{v}_1 + a_2\mathbf{v}_2 + a_3\mathbf{v}_3 + a_4\mathbf{v}_4 \tag{24}$$

where, $\mathbf{v}_1$, $\mathbf{v}_2$, $\mathbf{v}_3$, $\mathbf{v}_4$ are divergence, curl and deformation vector fields, and are described by:

$$\begin{aligned}
\mathbf{v}_1 &= x\frac{\partial}{\partial x} + y\frac{\partial}{\partial y} \\
\mathbf{v}_2 &= -y\frac{\partial}{\partial x} + x\frac{\partial}{\partial y} \\
\mathbf{v}_3 &= x\frac{\partial}{\partial x} - y\frac{\partial}{\partial y} \\
\mathbf{v}_4 &= y\frac{\partial}{\partial x} + x\frac{\partial}{\partial y}
\end{aligned} \tag{25}$$

and a_i $(i = 1, \cdots, 4)$ are the coefficients of these vector fields. The distortions of an image caused by these four components are shown in Fig. 4.

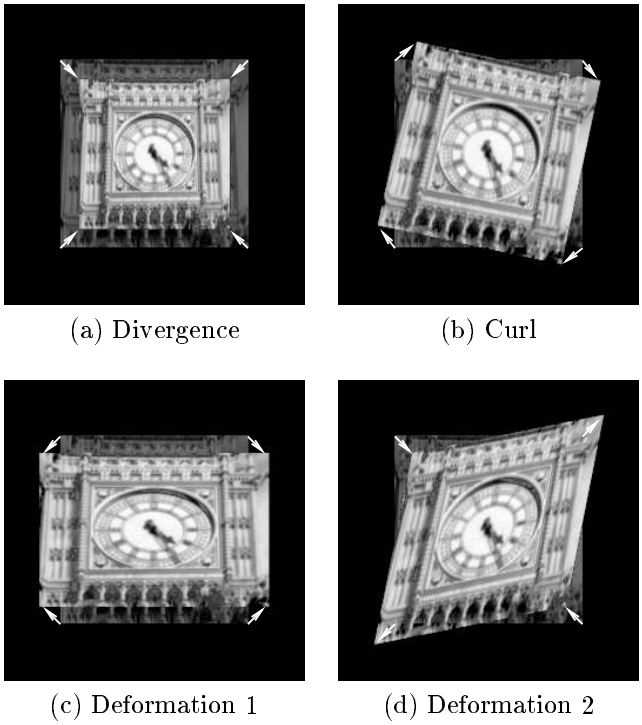

(a) Divergence (b) Curl

(c) Deformation 1 (d) Deformation 2

Figure 4: **Four components of an affine transformation.** We can observe how the square and the circle are distorted under the divergence, curl and two components of deformations.

4.2 Prolonged Affine Vector Field

We next apply the prolongation described in section 2.3, and derive prolonged affine vector fields.

From (4) and (25), the first order prolongations of divergence, $\mathbf{v}_1$, curl, $\mathbf{v}_2$, and two deformation vector fields,

$\mathbf{v}_3$ and $\mathbf{v}_4$, are computed by:

$$\begin{aligned}
\mathbf{v}_1{}^{(1)} &= x\frac{\partial}{\partial x} + y\frac{\partial}{\partial y} \\
\mathbf{v}_2{}^{(1)} &= -y\frac{\partial}{\partial x} + x\frac{\partial}{\partial y} + (1+y_x^2)\frac{\partial}{\partial y_x} \\
\mathbf{v}_3{}^{(1)} &= x\frac{\partial}{\partial x} - y\frac{\partial}{\partial y} - 2y_x\frac{\partial}{\partial y_x} \\
\mathbf{v}_4{}^{(1)} &= y\frac{\partial}{\partial x} + x\frac{\partial}{\partial y} + (1-y_x^2)\frac{\partial}{\partial y_x} \qquad (26)
\end{aligned}$$

where, as before y_x denotes the first derivative of y with respect to x. These are the vector fields in a three dimensional space whose coordinates are x, y and y_x as illustrated in Fig. 5 (a1), (b1), (c1) and (d1). The interpretation of these prolonged affine vector fields is as follows:

- **The prolonged divergence vector field (a1)** induces a flow which does not change in the y_x direction. Thus, the prolonged curve in this vector field does not move in the y_x direction meaning the tangential direction, φ, at each point on the original image curve does not change.
- **The prolonged curl vector field (b1)** induces an upward screw flow, meaning the tangential direction, φ, at any point on the original image curve increases monotonically.
- **The prolonged first deformation vector field (c1)** induces a downward flow if $y_x > 0$ and an upward flow if $y_x < 0$ approaching $y_x = 0$ asymptotically. This means the tangential direction, φ, at any point on the original image curve approaches $0°$ monotonically under this vector field.
- **The prolonged second deformation vector field (d1)** induces an upward flow if $-1 < y_x < 1$ and a downward flow if $y_x < -1$ or $1 < y_x$. Thus, if the tangential direction, φ, of the original image curve takes $-45° < \varphi < 45°$, then the direction increases, and if $\varphi < -45°$ or $45° < \varphi$ the direction decreases.

The projection of these vector fields onto the $x-y$ plane coincides with the original affine vector fields as shown in Fig. 5 (a2), (b2), (c2) and (d2).

Similarly, the second prolongations of the affine vector fields are computed from (5) and (25) as follows:

$$\begin{aligned}
\mathbf{v}_1^{(2)} &= x\frac{\partial}{\partial x} + y\frac{\partial}{\partial y} - y_{xx}\frac{\partial}{\partial y_{xx}} \\
\mathbf{v}_2^{(2)} &= -y\frac{\partial}{\partial x} + x\frac{\partial}{\partial y} + (1+y_x^2)\frac{\partial}{\partial y_x} + 3y_x y_{xx}\frac{\partial}{\partial y_{xx}} \\
\mathbf{v}_3^{(2)} &= x\frac{\partial}{\partial x} - y\frac{\partial}{\partial y} - 2y_x\frac{\partial}{\partial y_x} - 3y_{xx}\frac{\partial}{\partial y_{xx}} \\
\mathbf{v}_4^{(2)} &= y\frac{\partial}{\partial x} + x\frac{\partial}{\partial y} + (1-y_x^2)\frac{\partial}{\partial y_x} - 3y_x y_{xx}\frac{\partial}{\partial y_{xx}} \qquad (27)
\end{aligned}$$

These are the vector fields in a four dimensional space whose coordinates are x, y, y_x and y_{xx}, and the projection of these vector fields onto x, y and y_x coincides with the first order prolongation of the affine vector fields.

These prolonged vector fields will be used for investigating how the orientation, φ, arc-length, dv, and the curvature, κ, change under an affine transformation in the next section.

4.3 Orientation, Arc-Length and Curvature under Affine Transformations

We now investigate how the orientation of the tangent vector and the arc-length change under affine transformations.

By applying (26), we have the following Lie derivatives of φ and dv with respect to each basis vector field of affine transformations:

$$\begin{array}{ll}
\mathbf{v}_1{}^{(1)}[\varphi] = 0 & \mathbf{v}_3{}^{(1)}[\varphi] = -\sin 2\varphi \\
\mathbf{v}_2{}^{(1)}[\varphi] = 1 & \mathbf{v}_4{}^{(1)}[\varphi] = \cos 2\varphi \\
\mathbf{v}_1{}^{(1)}[dv] = dv & \mathbf{v}_3{}^{(1)}[dv] = \cos 2\varphi dv \\
\mathbf{v}_2{}^{(1)}[dv] = 0 & \mathbf{v}_4{}^{(1)}[dv] = \sin 2\varphi dv
\end{array} \qquad (28)$$

Similarly, we have the Lie derivatives of κ by using the second prolongations of affine vector fields as follows:

$$\begin{array}{ll}
\mathbf{v}_1{}^{(2)}[\kappa] = -\kappa & \mathbf{v}_3{}^{(2)}[\kappa] = -3\kappa\cos 2\varphi \\
\mathbf{v}_2{}^{(2)}[\kappa] = 0 & \mathbf{v}_4{}^{(2)}[\kappa] = -3\kappa\sin 2\varphi
\end{array} \qquad (29)$$

(28) and (29) show how the orientation, φ, the arc-length, dv, and the curvature, κ, are affected by divergence, curl and two components of deformation. Since as we have seen in (3) prolonged vector fields are linear, we have the change in orientation, $\delta\varphi$, the change in arc-length, δdv, and the change in curvature, $\delta\kappa$, caused by an affine transformation as follows:

$$\begin{aligned}
\delta\varphi &= \mathbf{v}^{(1)}[\varphi] \\
&= a_1\mathbf{v}_1^{(1)}[\varphi] + a_2\mathbf{v}_2^{(1)}[\varphi] + a_3\mathbf{v}_3^{(1)}[\varphi] + a_4\mathbf{v}_4^{(1)}[\varphi] \\
&= a_2 - a_3\sin 2\varphi + a_4\cos 2\varphi \qquad (30)
\end{aligned}$$

$$\begin{aligned}
\delta dv &= \mathbf{v}^{(1)}[dv] \\
&= a_1\mathbf{v}_1^{(1)}[dv] + a_2\mathbf{v}_2^{(1)}[dv] + a_3\mathbf{v}_3^{(1)}[dv] + a_4\mathbf{v}_4^{(1)}[dv] \\
&= (a_1 + a_3\cos 2\varphi + a_4\sin 2\varphi)dv \qquad (31)
\end{aligned}$$

$$\begin{aligned}
\delta\kappa &= \mathbf{v}^{(2)}[\kappa] \\
&= a_1\mathbf{v}_1^{(2)}[\kappa] + a_2\mathbf{v}_2^{(2)}[\kappa] + a_3\mathbf{v}_3^{(2)}[\kappa] + a_4\mathbf{v}_4^{(2)}[\kappa] \\
&= (-a_1 - 3a_3\cos 2\varphi - 3a_4\sin 2\varphi)\kappa \qquad (32)
\end{aligned}$$

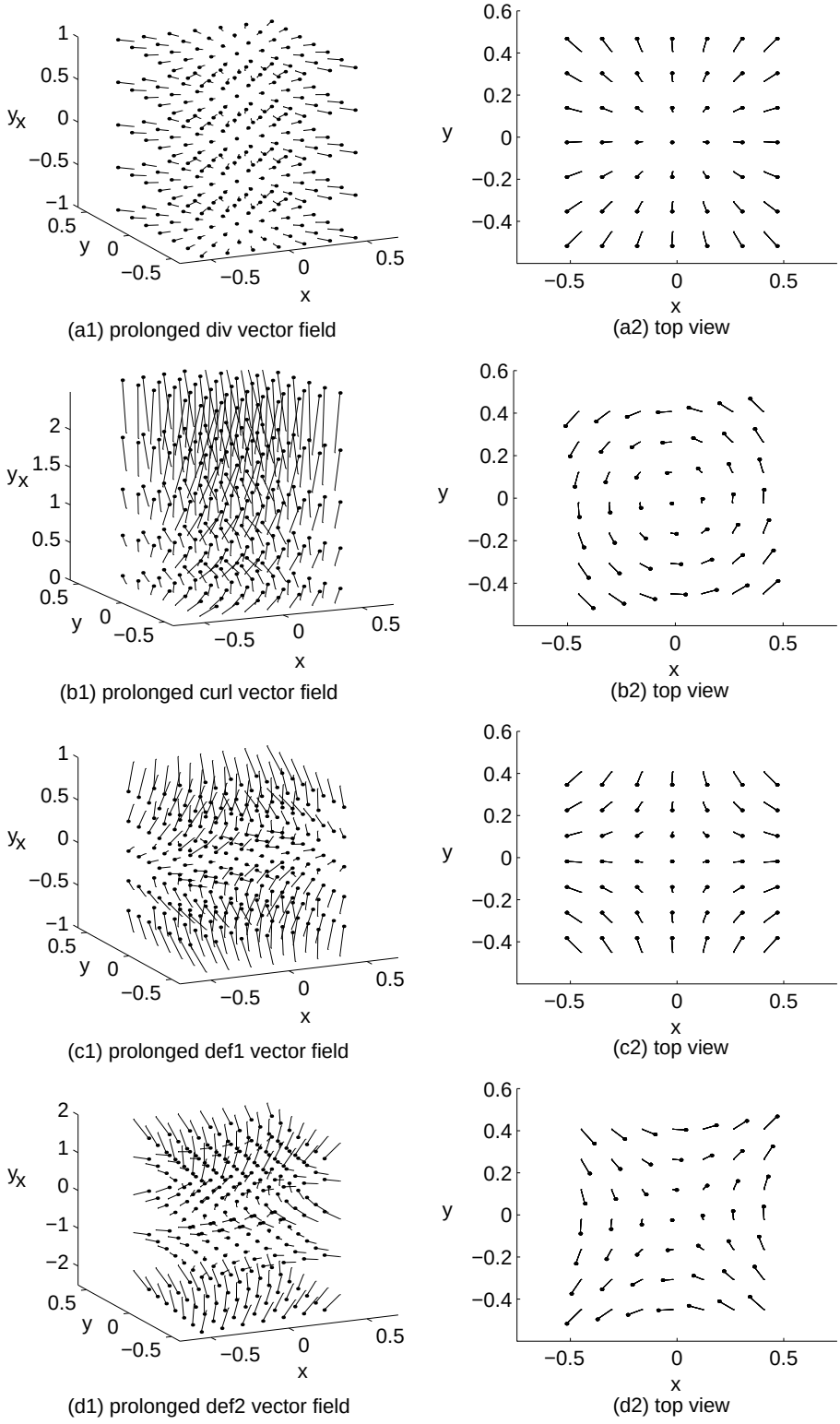

Figure 5: **Prolonged affine vector fields and their top view.**

Note that the change in orientation is made up of the curl and deformation components, and is not affected by the divergence component; the changes in arc-length and curvature are made up of the divergence and deformation components, and is not affected by the curl component.

4.4 Change in Directional Moments under Affine Transformations

In the last section, we have investigated how the change in orientation and the change in arc-length are described by the four components of an affine transformation. We now apply these results and derive the relationship between the change in moments of orientation and the affine transformation.

Suppose the function F is a trigonometric function of orientation φ. Substituting trigonometric functions of φ for F in (16) and substituting (30) and (31) into (19) and (20), we derive the relationship between the change in nth order directional moments and the coefficients, $a_i (i = 1, \cdots, 4)$, of affine vector fields as follows:

$$\begin{bmatrix} \delta I_{\sin n\varphi} \\ \delta I_{\cos n\varphi} \end{bmatrix} = \begin{bmatrix} m^n_{11}, m^n_{12}, m^n_{13}, m^n_{14} \\ m^n_{21}, m^n_{22}, m^n_{23}, m^n_{24} \end{bmatrix} \begin{bmatrix} a_1 \\ a_2 \\ a_3 \\ a_4 \end{bmatrix} \quad (33)$$

where:

$$\begin{aligned}
m^n_{11} &= I_{\sin n\varphi} \\
m^n_{12} &= nI_{\cos n\varphi} \\
m^n_{13} &= ((n+1)I_{\sin (n-2)\varphi} - (n-1)I_{\sin (n+2)\varphi})/2 \\
m^n_{14} &= ((n+1)I_{\cos (n-2)\varphi} + (n-1)I_{\cos (n+2)\varphi})/2 \\
m^n_{21} &= I_{\cos n\varphi} \\
m^n_{22} &= -nI_{\sin n\varphi} \\
m^n_{23} &= ((n+1)I_{\cos (n-2)\varphi} - (n-1)I_{\cos (n+2)\varphi})/2 \\
m^n_{24} &= (-(n+1)I_{\sin (n-2)\varphi} - (n-1)I_{\sin (n+2)\varphi})/2
\end{aligned}$$

Note that the change in moments of orientation can be described by simple linear combinations of the moments of orientation and the coefficients of affine vector fields.

If we have the directional moments in two different orders, i.e. $n = 2$ and $n = 4$, then four coefficients, a_i $(i = 1, \cdots, 4)$, can be computed uniquely from:

$$\begin{bmatrix} \delta I_{\sin 2\varphi} \\ \delta I_{\cos 2\varphi} \\ \delta I_{\sin 4\varphi} \\ \delta I_{\cos 4\varphi} \end{bmatrix} = \begin{bmatrix} m^2_{11}, m^2_{12}, m^2_{13}, m^2_{14} \\ m^2_{21}, m^2_{22}, m^2_{23}, m^2_{24} \\ m^4_{11}, m^4_{12}, m^4_{13}, m^4_{14} \\ m^4_{21}, m^4_{22}, m^4_{23}, m^4_{24} \end{bmatrix} \begin{bmatrix} a_1 \\ a_2 \\ a_3 \\ a_4 \end{bmatrix} \quad (34)$$

4.5 Change in Curvature Moments under Affine Transformations

We next investigate how the curvature moments change under affine vector fields. Substituting (28) and (29) into (22), we have the change in curvature moments under affine vector fields:

$$\begin{aligned}
\delta I_{\kappa^n} \;=\; & (1-n)a_1 I_{\kappa^n} + (1-3n)a_3 I_{\kappa^n \cos 2\varphi} \\
& + (1-3n)a_4 I_{\kappa^n \sin 2\varphi} \qquad (35)
\end{aligned}$$

This means by choosing $n = \frac{1}{3}$, $n = 1$ and $n = 2$ in (35), we have the following simple relationship between the change in curvature moments and the coefficients of affine vector fields:

$$\begin{bmatrix} \delta I_{\kappa^{\frac{1}{3}}} \\ \delta I_{\kappa} \\ \delta I_{\kappa^2} \end{bmatrix} = \begin{bmatrix} \frac{2}{3} I_{\kappa^{\frac{1}{3}}} & 0 & 0 \\ 0 & -2I_{\kappa \cos 2\varphi} & -2I_{\kappa \sin 2\varphi} \\ -I_{\kappa^2} & -5I_{\kappa^2 \cos 2\varphi} & -5I_{\kappa^2 \sin 2\varphi} \end{bmatrix} \begin{bmatrix} a_1 \\ a_3 \\ a_4 \end{bmatrix} \quad (36)$$

Thus, divergence, a_1, and deformation, a_3 and a_4, are computed uniquely from the change in curvature moments. The interesting properties of curvature moments are as follows:

1. The change in $I_{\kappa^{\frac{1}{3}}}$ is irrelevant to the deformation and rotation components of an affine transformation. Thus, divergence component, a_1, can be computed simply from the change in $I_{\kappa^{\frac{1}{3}}}$.
2. The change in I_κ is irrelevant to the divergence and rotation components of an affine transformation.
3. The rotation component, a_2, cannot be determined from curvature moments.

5 Experiments

5.1 Implementation

Up to now we have described the theoretical framework of a method for computing group transformations from the change in image moments. In this section, we describe how to implement the method.

If the texture pattern in an image is simple, then we can compute image moments from the parameterised curves fitted to edge data or gray scale images. The procedure of this is as follows:

1. We first extract edge points in images by using the Canny edge detector [5].
2. The B-spline curves are fitted to the Canny edge data by using the MDL-based curve fitting algorithm proposed by Cham and Cipolla [6].
3. The directional moments ($n = 2, 4$) defined in (17) and (18) or the curvature moments ($n = \frac{1}{3}, 1, 2$) defined in (21) are computed from the parameterised curves.

4. The affine transformation is computed from these moments by using (34).

If the image is highly textured, we cannot fit parameterised curves in general. In such cases, we use the image moments based on the discrete sampling at every edge point. Consider the image measurement, $\boldsymbol{q}^T = [\varphi, \nu]$, which consists of the measured orientation, φ, and the measured length, ν, of a texture segment at each edge point. If we have r sampling points, $\boldsymbol{x}_i (i = 1, \cdots, r)$, on an image curve, C, then the discrete approximation of the image moments can be described as follows:

$$I \simeq \sum_{i=1}^{r} F(\boldsymbol{x}_i)\nu(\boldsymbol{x}_i)$$

where, $F(\boldsymbol{x}_i)$ and $\nu(\boldsymbol{x}_i)$ are the values of the function F and the length ν at the image point $\boldsymbol{x}_i$.

5.2 Extracting Affine Transformations

In this section, we demonstrate the accuracy of the extracted affine transformations.

Fig. 6 shows images used in this experiment and the results of estimating surface motions. The images in the first and second columns in Fig. 6 show the original images of various texture patterns and the distorted images after affine transformations. The affine transformations extracted by the directional moment method proposed in this paper are shown by flows in the images in the second column. The calibrated affine transformations are shown in the third column. The results are qualitatively good even for highly textured images. This is because the proposed method does not require correspondences of individual image features. Unlike the methods based on spatiotemporal gradients of image intensity [1], the amount of visual motion allowed is relatively large as shown in these images. The proposed method however requires the area of interest between the two images to be identified.

5.3 Visual Navigation from Image Moments

To demonstrate the usefulness of the proposed method, we in this section exploit the proposed method in the realtime visual guidance of a robot. We first show how a moving observer can determine the object surface orientation and time to contact from the affine transformation estimated from image moments. The relations between the motion parameters and the surface position and orientation were presented in [7, 15].

Consider a 3D point $\boldsymbol{P}$ to be projected onto a unit image sphere, Σ, so that $\boldsymbol{P}$ is specified by a unit vector $\boldsymbol{Q}$ and the depth λ to the point from the viewer center (see Fig. 7).

$$\boldsymbol{P} = \lambda \boldsymbol{Q}$$

Let x and y be the horizontal and the vertical axes of an image plane tangent to the image sphere at $\boldsymbol{Q}$, and z be the axis lying in viewing direction. Suppose the viewer is moving with translational velocity of $\boldsymbol{U} = [U_1, U_2, U_3]$ and rotational velocity of $\boldsymbol{\Omega} = [\Omega_1, \Omega_2, \Omega_3]$ with respect to the above coordinates. It is convenient to consider the three dimensional configurations projected onto the image, that is the translational velocity component parallel to the image plane scaled by the depth, λ:

$$\boldsymbol{B} = \frac{1}{\lambda}[U_1, U_2]$$

and the depth gradient component of a surface scaled by depth:

$$\boldsymbol{F} = \frac{1}{\lambda}[\lambda_x, \lambda_y]$$

where, λ_x and λ_y denote the derivatives of λ with respect to x and y respectively. Thus, the direction and the magnitude of $\boldsymbol{F}$ are equal to the tilt angle, ψ, and the tangent of the slant angle, ϕ, of the surface as follows:

$$\angle \boldsymbol{F} = \psi \quad (37)$$

$$|\boldsymbol{F}| = \tan\phi \quad (38)$$

where, $\angle \boldsymbol{F}$ and $|\boldsymbol{F}|$ are the angle and the magnitude of $\boldsymbol{F}$.

It is well known that the relations between the shape, motion and the coefficients of affine vector fields, $a_i, (i = 1, \cdots, 4)$, are given by [7, 15]:

$$a_1 = \frac{\langle \boldsymbol{U}, \boldsymbol{Q} \rangle}{\lambda} + \frac{1}{2}\langle \boldsymbol{F}, \boldsymbol{B} \rangle \quad (39)$$

$$a_2 = -\langle \boldsymbol{\Omega}, \boldsymbol{Q} \rangle + \frac{1}{2}[\boldsymbol{F}, \boldsymbol{B}] \quad (40)$$

$$(a_3^2 + a_4^2)^{\frac{1}{2}} = \frac{1}{2}|\boldsymbol{F}||\boldsymbol{B}| \quad (41)$$

where, $\langle \boldsymbol{u}_1, \boldsymbol{u}_2 \rangle$ denotes a scalar product of two vectors, $\boldsymbol{u}_1$ and $\boldsymbol{u}_2$, and $[\boldsymbol{u}_1, \boldsymbol{u}_2]$ denotes the determinant of a matrix consisting of two vectors, $\boldsymbol{u}_1$ and $\boldsymbol{u}_2$. The axis of deformation (or the direction of maximum expansion), μ, bisects $\boldsymbol{B}$ and $\boldsymbol{F}$ [15] as follows:

$$\mu = \frac{\angle \boldsymbol{B} + \angle \boldsymbol{F}}{2} \quad (42)$$

As shown in the previous work [7], we can obtain partial solutions to the 3D motion of the observer and the structure of the scene from these relations. For example,

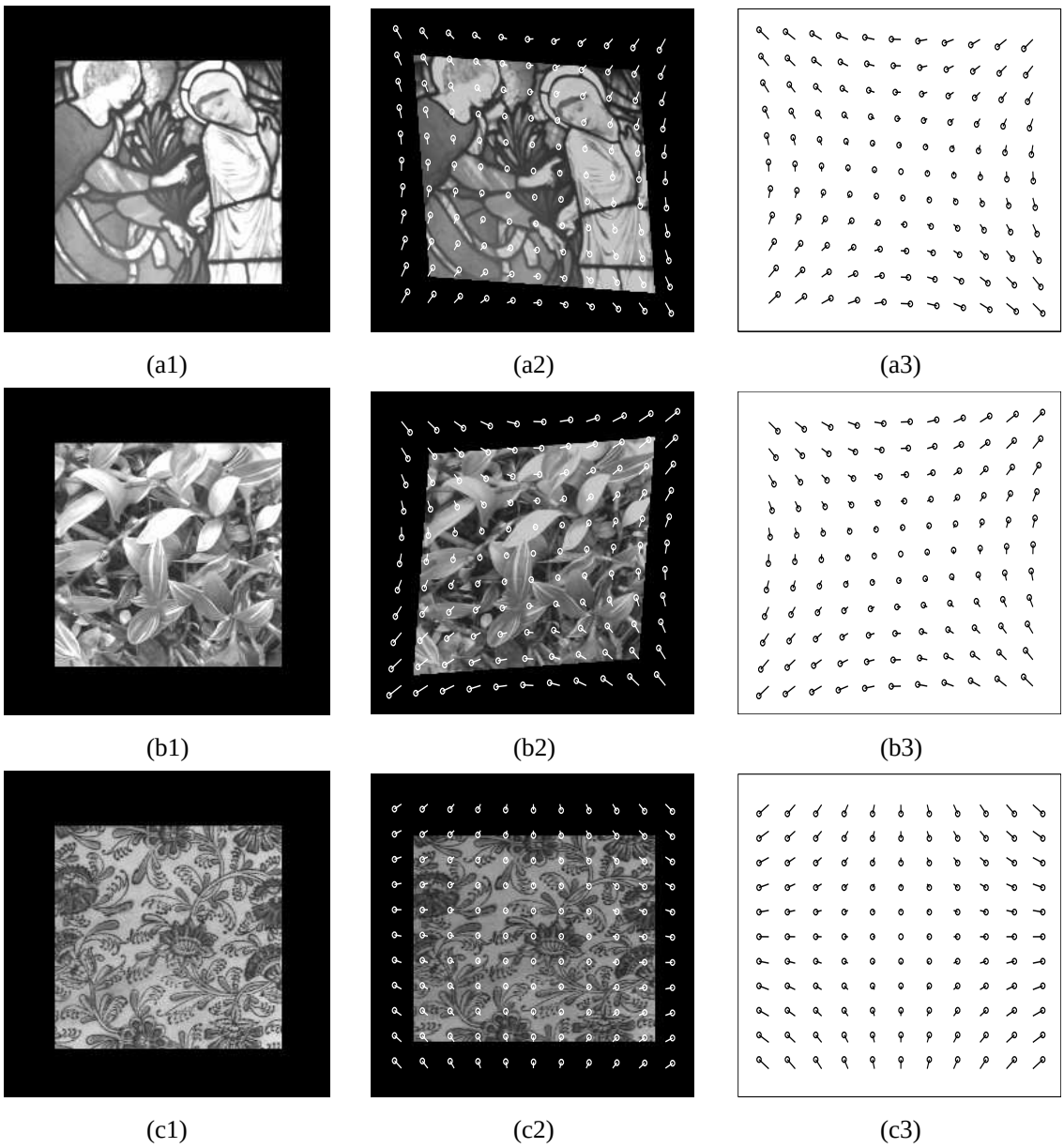

Figure 6: **Extracting Affine Transformations.** Images in the first and second columns are the original and the affinely transformed images. The affine flows estimated by the proposed method are shown in the images in the second column. The calibrated affine flows are shown in the third column. Examples include (a) stained glass window, (b) leaves and (c) a cloth with texture.

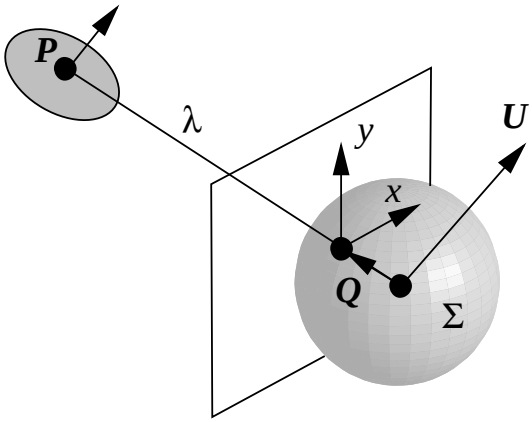

(a) projection

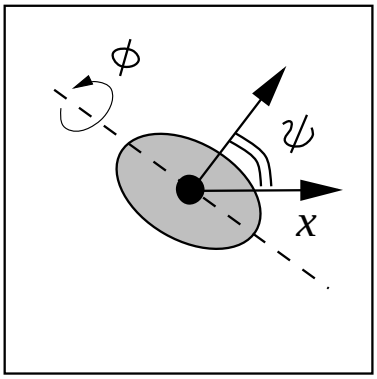

(b) image

Figure 7: **3D configuration.** The point $\boldsymbol{P}$ is specified by a unit vector, $\boldsymbol{Q}$, and the depth, λ. The disk is projected onto the plane tangent to the image sphere, Σ, at $\boldsymbol{Q}$. The orientation of the disk is specified by the slant angle, ϕ, and the tilt angle, ψ.

if we know the direction of motion of the observer, $\angle \boldsymbol{B}$, we can compute the tilt angle, ψ, of the surface from (37) and (42). Then, we can compute the rotational and translational motion of the observer from (40), (39) and (41). The second observation is very important for visual navigation, since it is directly related to the time-to-contact, t_c, to the surface as follows:

$$t_c = \frac{\lambda}{\langle \boldsymbol{U}, \boldsymbol{Q} \rangle}$$

If we also know the magnitude of the motion of the observer, $|\boldsymbol{B}|$, we can extract the slant, ϕ, of the object surface from (41) and (38). By using the coefficients, $a_i (i = 1, \cdots, 4)$, of affine vector fields extracted from the changes in moments (34), time-to-contact, t_c, 2D rotation of the viewer, θ, slant, ϕ and tilt ψ are computed from the following equations:

$$\begin{aligned} \frac{1}{t_c} &= a_1 - a_3 \cos 2\angle \boldsymbol{B} - a_4 \sin 2\angle \boldsymbol{B} \\ \theta &= -a_2 + a_4 \cos 2\angle \boldsymbol{B} - a_3 \sin 2\angle \boldsymbol{B} \\ \tan\phi &= \frac{2}{|\boldsymbol{B}|}(a_3^2 + a_4^2)^{\frac{1}{2}} \\ \psi &= 2\mu - \angle \boldsymbol{B} \end{aligned} \tag{43}$$

Although we do not know the absolute distance to the surface, the computed slant, tilt and time-to-contact are sometimes sufficient for robot navigation. In this experiment, a robot with a camera is navigated to an unknown surface, so that the robot lands on to the surface safely at the right angle to the surface. The computed slant and tilt angles are used to control the posture of the robot, and the time-to-contact is used to stop the robot just in front of the surface.

Fig. 8 (a) shows the horizontal and vertical motion of the robot with a camera. These motion causes distortion in the image as shown in Fig. 8 (b) and (c), and the affine distortion is measured from the change in directional moments as described in this paper. The computed distortions are used to derive time-to-contact and the orientation of the object surface from (43). The computed axis of deformation and orientation of the surface is shown in Fig. 8 (c) and (d). As shown in Fig. 8 (e), the robot is controlled in realtime according to this information and is made to land on the object surface at the right angle to the surface. All necessary information for landing can be computed from the changes in moment in images, and no correspondence of individual image features is required.

6 Discussion

We now summarise and discuss the properties of the proposed method for extracting group transformations.

1. **Correspondence:**
   Since the proposed method does not require any correspondence of individual image features, group transformations can be computed even for highly textured images. The correspondence-based methods sometimes fail catastrophically due to a small number of incorrect correspondences. The proposed method however requires the area of interest between two images to be identified. We should also note that the research for improving the performance of correspondence based methods is also active [2, 18, 27, 30].

2. **The Class of Transformations:**
   Although moment based methods have been studied

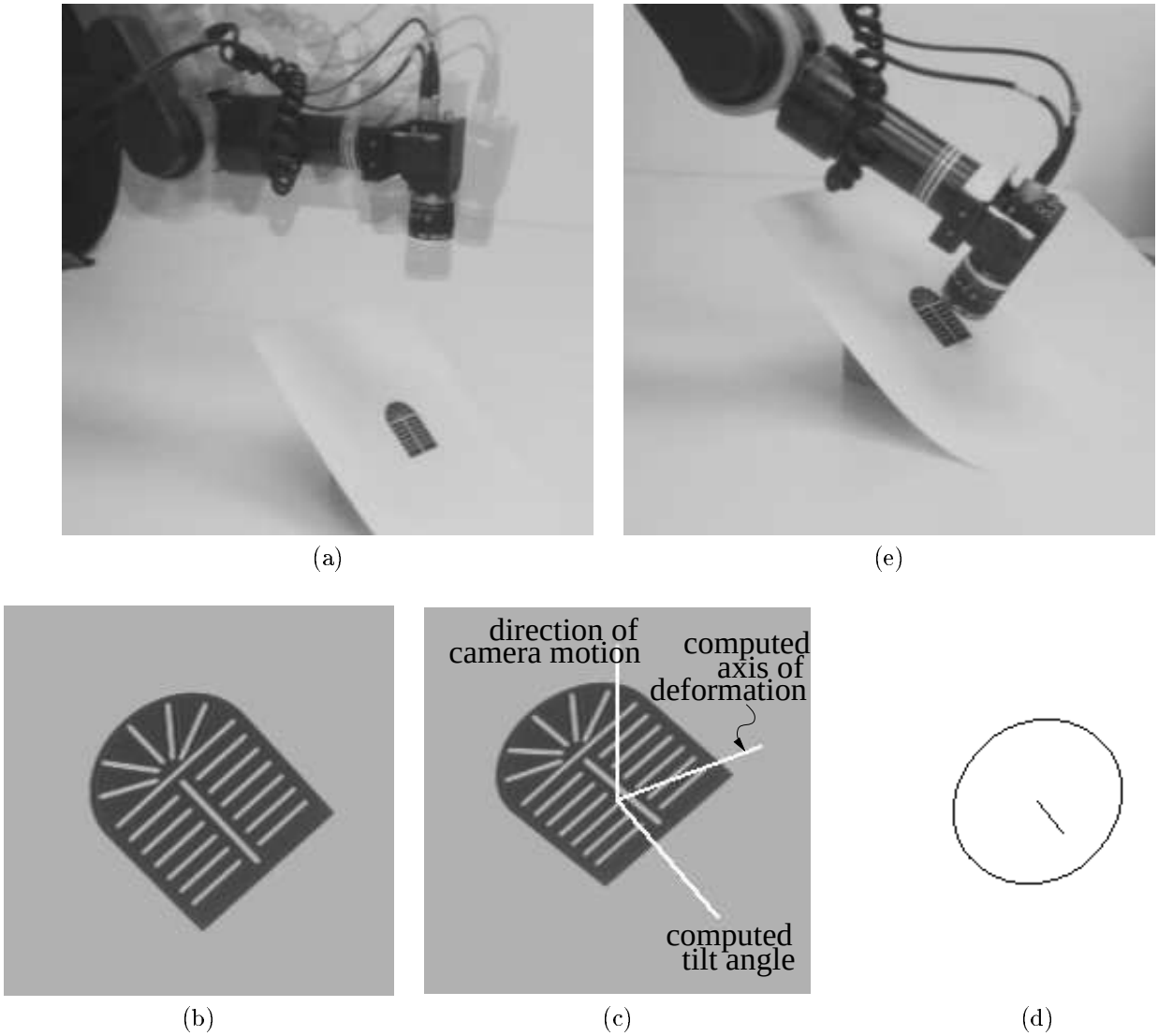

Figure 8: **Landing using the affine transform.** (a) shows inspection of time-to-contact and the orientation of surface. (b) and (c) show example images extracted during the camera motion. The tilt angle of the surface is estimated from the direction of camera translation, A, projected in an image, and the axis of deformation, μ, computed from the proposed method, and is shown in (c) by the white line. (d) shows computed slant and tilt angles using an oriented circle and a normal. As shown in (e), the robot uses the extracted tilt, slant and time-to-contact to land on the surface at a right angle in realtime.

previously [7, 12], these methods are limited to specific transformation groups, such as the affine group. The proposed method is general and can be applied for extracting transformations in various Lie groups such as Euclidean, similarity and projective groups. This is done, by simply substituting the basis vector fields of these transformation groups into (16) instead of the affine vector fields.

3. **The Class of Texture Patterns:**
The methods based on area moments [7, 12] require closed curves to be extracted in images, while the method based on directional or curvature moments does not require the curves in images to be closed. Thus the method based on these moments can be applied to images with a wider class of texture patterns.

References

[1] P. Anandan. A computational framework and an algorithm for the measurement of visual motion. *International Journal of Computer Vision*, Vol. 2, No. 3, pp. 283–310, 1989.

[2] P. Beardsley, P. Torr, and A. Zisserman. 3D model acquisition from extended image sequences. In B.F. Buxton and R. Cipolla, editors, *Proc. 4th European Conference on Computer Vision*, Vol. 2, (LNCS 1064), pp. 683–695, Cambridge, 1996. Springer–Verlag.

[3] J.R. Bergen, P. Anandan, K.J. Hanna, and R. Hingorani. Hierarchical model-based motion estimation. In G. Sandini, editor, *Proc. 2nd European Conference on Computer Vision*, pp. 237–252, Santa Margherita, Italy, 1992. Springer–Verlag.

[4] A. Blake and C. Marinos. Shape from texture: estimation, isotropy and moments. *Artificial Intelligence*, Vol. 45, pp. 323–380, 1990.

[5] J.F. Canny. A computational approach to edge detection. *IEEE Trans. Pattern Analysis and Machine Intelligence*, Vol. 8, pp. 679–698, 1986.

[6] T.J. Cham and R. Cipolla. Automated B-spline curve representation with MDL-based active contours. In *Proc. 7th British Machine Vision Conference*, Vol. 2, pp. 363–372, Edinburgh, September 1996.

[7] R. Cipolla and A. Blake. Surface orientation and time to contact from image divergence and deformation. In G. Sandini, editor, *Proc. 2nd European Conference on Computer Vision*, pp. 187–202, Santa Margherita, Italy, 1992. Springer–Verlag.

[8] B. Duc. Motion estimation using invariance under group transformations. In *Proc. 12th International Conference on Pattern Recognition*, pp. 159–163, Jerusalem, Israel, 1994.

[9] J. Garding. Shape from texture and contour by weak isotropy. *Artificial Intelligence*, Vol. 64, pp. 243–297, 1993.

[10] N. Jacobson. *Lie algebras*. New York, 1962.

[11] T. Kanade and J.R. Kender. Mapping image properties into shape constraints: Skewed symmetry, affine-transformable patterns, and the shape-from-texture paradigm. In J. Beck et al, editor, *Human and Machine Vision*, pp. 237–257. Academic Press, NY, 1983.

[12] K. Kanatani. Detecting the motion of a planar surface by line and surface integrals. *Computer Vision, Graphics and Image Processing*, Vol. 29, pp. 13–22, 1985.

[13] K. Kanatani. Structure and motion from optical flow under orthographic projection. *Computer Vision, Graphics and Image Processing*, Vol. 35, pp. 181–199, 1986.

[14] K. Kanatani. *Group-Theoretical Methods in Image Understanding*. Springer-Verlag, 1990.

[15] J.J. Koenderink. Optic flow. *Vision Research*, Vol. 26, No. 1, pp. 161–180, 1986.

[16] J.J. Koenderink and A.J. van Doorn. Invariant properties of the motion parallax field due to the movement of rigid bodies relative to an observer. *Optica Acta*, Vol. 22, No. 9, pp. 773–791, 1975.

[17] J.J. Koenderink and A.J. van Doorn. Geometry of binocular vision and a model for stereopsis. *Biological Cybernetics*, Vol. 21, pp. 29–35, 1976.

[18] J.M. Lawn and R. Cipolla. Reliable extraction of the camera motion using constraints on the epipole. In B.F. Buxton and R. Cipolla, editors, *Proc. 4th European Conference on Computer Vision*, Vol. 2, (LNCS 1064), pp. 161–173, Cambridge, England, 1996. Springer–Verlag.

[19] K.V. Mardia. *Statistics of directional data*. Academic Press, London, 1972.

[20] T. Moons, E.J. Pauwels, L.J. Van Gool, and A. Oosterlinck. Foundations of semi-differential invariants. *International Journal of Computer Vision*, Vol. 14, pp. 25–47, 1995.

[21] J.L. Mundy and A. Zisserman. *Geometric Invariance in Computer Vision*. MIT Press, Cambridge, USA, 1992.

[22] D. Murray and B. Buxton. *Experiments in the machine interpretation of visual motion*. MIT Press, Cambridge, USA, 1990.

[23] P.J. Olver. *Applications of Lie Groups to Differential Equations*. Springer-Verlag, 1986.

[24] J. Sato. *Group Invariance in the Visual Motion and Matching of Curves*. PhD thesis, University of Cambridge, 1996.

[25] J. Sato and R. Cipolla. Image registration using multi-scale texture moments. *Image and Vision Computing*, Vol. 13, No. 5, pp. 341–353, 1995.

[26] H.S. Sawhney and A.R. Hanson. Identification and 3D description of 'shallow' environmental structure in a sequence of images. In *Proc. Conference on Computer Vision and Pattern Recognition*, pp. 179–185, Lahaina, 1991.

[27] P. Torr. Motion segmentation and outlier detection. PhD thesis, University of Oxford, 1995.

[28] L.J. Van Gool, T. Moons, D. Ungureanu, and A. Oosterlinck. The characterization and detection of skewed symmetry. *Computer Vision and Image Understanding*, Vol. 61, No. 1, pp. 138–150, 1995.

[29] L.J. Van Gool, E. Pauwels, and A. Oosterlinck. Vision and Lie's approach to invariance. *Image and Vision Computing*, Vol. 13, No. 4, pp. 259–277, 1995.

[30] Z. Zhang, R. Deriche, O. Faugeras, and Q.T. Luong. A robust technique for matching two uncalibrated images through the recovery of the unknown epipolar geometry. *Artificial Intelligence*, Vol. 78, No. 1, pp. 87–119, 1995.